

W pair production in e^+e^- annihilation: Radiative corrections including hard bremsstrahlung

J. Fleischer and K. Kołodziej*

Fakultät für Physik, Universität Bielefeld, D-4800 Bielefeld 1, Germany

F. Jegerlehner

Paul Scherrer Institute, CH-5232 Villigen PSI, Switzerland

(Received 23 March 1992; revised manuscript received 5 August 1992)

A calculation of the hard bremsstrahlung process $e^+e^- \rightarrow W^+W^-\gamma$ is presented and combined with previous results for the electroweak radiative corrections to $e^+e^- \rightarrow W^+W^-$ (including soft bremsstrahlung). The phase space integrations are performed by the Monte Carlo method which allows one to apply cuts in the photon phase space. Results are given for the total cross section (no cuts) as well as for cuts in the photon energy and the angle between the photon momentum and the beam axis. The full $O(\alpha)$ calculation is improved by including the known leading logarithmic $O(\alpha^2)$ contributions. The dependence of the results on the renormalization scheme (α and G_μ scheme) is investigated.

PACS number(s): 13.40.Ks, 13.10.+q, 14.80.Er

I. INTRODUCTION

W pair production, which will be the dominating process at the CERN e^+e^- collider LEP 200, presents an optimal possibility for a first direct clean observation of gauge-field self-interactions (Yang-Mills couplings), since the total W pair production cross section is very sensitive to the triple gauge couplings [1]. These couplings are required by local non-Abelian gauge invariance, and before they have been confirmed, the gauge-boson nature of the vector bosons W and Z remains a hypothesis.

Although the electroweak standard model (SM) works perfectly even at the level of quantum corrections [2], a direct test of the existence of the $SU(2)_L$ Yang-Mills couplings is still missing. In W pair production, the contributions which depend on the triple gauge couplings, the s -channel Z - and γ -exchange terms, are suppressed at threshold and grow fast with the beam energy. It is therefore very important to run at the highest accessible energies for precise tests of these couplings. For example, at 170 (197.5) GeV the dominating t -channel ν exchange contributes 121.5% (200.0%), while the Z exchange yields -13.1% (-59.8%) and γ exchange -8.5% (-40.2%) to the total cross section at tree level. The numbers in parentheses are the values at the peak of the Born cross section. Since the Z - and γ -exchange contributions are of similar size and substantially smaller than the t -channel contribution, a precise investigation is necessary in order to be able to disentangle the ZWW and the γWW couplings. A very good test of the SM gauge couplings (and the gauge cancellation mechanism at work) is possible by a precise location of the peak of the total cross section. Unfortunately, because of the limitation in energy at LEP 200, this peak can be tested only at some future e^+e^- collider.

Substantial improvement on the precision measurements of the W mass and width will be possible. These measurements will be confronted with the theoretical predictions of the SM, such as, e.g., the M_W - M_Z relation (see, e.g., [3]), and thus provide bounds or signals on possible *new physics*. Note that, given the LEP value for M_Z , the present top-quark mass bounds essentially derive from the W mass measurements at the hadron colliders [4].

Our aim is to control the SM prediction with an accuracy of better than 1%, which requires a careful study of higher-order effects. The physically interesting *weak effects* have to be clearly disentangled from the large QED corrections which are common to any $G \otimes U(1)_{em}$ theory. This requires both a precise theoretical understanding, in particular, of the QED corrections and experimentally a precise control of the beam properties, detector efficiencies, and phase-space cuts, which requires simulation by Monte Carlo event generators.

The electroweak radiative corrections for the process $e^+e^- \rightarrow W^+W^-$, including the virtual effects and soft-photon emission to order $O(\alpha)$, were calculated by several authors [5–8]. In particular, the results of Refs. [7] and [8] are in excellent agreement. In Ref. [8] two different renormalization schemes (α and G_μ schemes) have been employed. In both schemes the vector-boson masses M_W and M_Z and a coupling are used as input parameters. The two schemes differ in the choice of the coupling parameter: Either the fine-structure constant α or the Fermi constant G_μ may be used. As has been discussed in Ref. [8], the counterterms for the electroweak radiative corrections have to be chosen differently in both cases.

The hard bremsstrahlung process $e^+e^- \rightarrow W^+W^-\gamma$ was calculated a long time ago in Ref. [9]. Here we calculate this process using the general method which was described in Ref. [10] (where also fermion annihilation into other channels was discussed). The hard bremsstrahlung for W pair production has also been calculated in Ref. [11]. The results in the two approaches agree per-

*On leave from the Institute of Physics, University of Silesia, 40-007 Katowice, ul. Uniwersytecka 4, Poland.

fectly. However, the comparison of the hard bremsstrahlung calculations showed that the numerical sandwiching of γ operators between helicity spinors [10] is much faster in computer time than the numerical evaluation of analytic expressions obtained by means of the Weyl–van der Waerden formalism [15].

In our approach we have found very good agreement between the α and G_μ schemes. Strictly speaking, this is true only because the top-quark mass m_t and Higgs-boson mass m_H have been chosen to be constrained by the relationship between α , G_μ , M_Z , and M_W [3]. For arbitrary values of m_t , large discrepancies may be obtained (see Ref. [16] for a detailed discussion of this point). The remaining scheme dependence of the results can be attributed to the neglected higher-order corrections.

II. W PAIR PRODUCTION PROCESS

The calculation of virtual (loop) and soft-photon corrections for the process $e^+e^- \rightarrow W^+W^-$, on which the present work is based, was extensively discussed in Ref. [8]. Besides the physically most interesting virtual corrections, the bremsstrahlung emitted from the charged particles has to be taken into account in a manner convenient for the comparison with an actual experiment. The bremsstrahlung diagrams are depicted in Fig. 1. Commonly, one distinguishes between the QED corrections [to order $O(\alpha)$ given by the diagrams with one additional photon line, virtual or real, attached to the Born diagrams] and the genuine “weak” corrections which depend on the top-quark and Higgs-boson masses and could be affected by physics beyond the SM. In our case this subdivision is not gauge invariant because of the non-Abelian nature of the final-state particles.

In practice, the bremsstrahlung is divided into a soft ($E_\gamma < \omega$) and a hard ($E_\gamma > \omega$) part because of the cancellation of the infrared-divergent contributions (and the large Sudakov double logarithms) among the virtual photonic corrections and the soft bremsstrahlung. The “cutoff” energy ω is arbitrary, but must be chosen smaller than E_γ^{\min} , the threshold energy for photon detection of the experimental apparatus. In order to be able to apply appropriate cuts in the photon phase space, the hard bremsstrahlung is evaluated by performing a phase-space integration with the help of a Monte Carlo (MC) routine. It has been checked numerically that the total cross section is independent of the cutoff ω for sufficiently small ω .

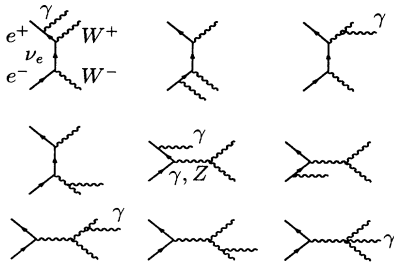


FIG. 1. Bremsstrahlung diagrams for $e^+e^- \rightarrow W^+W^-$ in the unitary gauge.

We write the differential cross section as a sum of the one-loop corrected plus the $O(\alpha)$ soft bremsstrahlung part ($h_e = \text{electron helicity}$):

$$\frac{d\sigma(h_e; \lambda, \bar{\lambda}; < \omega)}{d(\cos\Theta)} = \frac{d\sigma(h_e; \lambda, \bar{\lambda})}{d(\cos\Theta)} + \frac{d\sigma_0(h_e; \lambda, \bar{\lambda})}{d(\cos\Theta)} C_{\text{Br}}(\omega), \quad (1)$$

where

$$\frac{d\sigma(h_e; \lambda, \bar{\lambda})}{d(\cos\Theta)} = \frac{\beta_W}{32\pi s} |M|^2. \quad (2)$$

M is the $e^+e^- \rightarrow W^+W^-$ transition matrix element to order $O(\alpha)$, $s = 4E_b^2$ ($E_b = \text{beam energy in the c.m. system}$) and $\beta_W = (1 - 4M_W^2/s)^{1/2} = p/E_b$, p being the magnitude of the W three-momentum.

The soft bremsstrahlung factorizes for small photon energies ($E_\gamma = |\mathbf{k}| \leq \omega \ll E_b$) into the Born differential cross section and the bremsstrahlung integral C_{Br} (see [8]). The hard bremsstrahlung, to be added to (1) may be written as

$$\frac{d\sigma_h(h_e; \lambda, \bar{\lambda}; > \omega)}{d(\cos\Theta)} = \frac{\alpha}{4\pi s} \int_{k>\omega} \frac{pk d\Omega_\gamma}{\sqrt{s-k+E_W k \cos\delta/p}} |M_{\text{Br}}|^2, \quad (3)$$

with $k = |\mathbf{k}|$, $E_W = (p^2 + M_W^2)^{1/2}$, and δ denotes the angle between \mathbf{p}_{W^-} and \mathbf{k} . M_{Br} is the transition matrix element for $e^+e^- \rightarrow W^+W^- \gamma$, which can be parametrized in the α or G_μ scheme. The integral is performed over photon phase space with $k > \omega$ by means of the Monte Carlo routine VEGAS [17]. The random numbers are generated according to the distribution

$$\frac{1}{k(1 - \beta_e^2 \cos^2\Theta_\gamma)}, \quad (4a)$$

where Θ_γ is the angle between \mathbf{k} and the beam axis and $\beta_e = (1 - 4m_e^2/s)^{1/2}$. For the calculation of the total cross section, we perform the integration over $\cos\Theta$ in (3) using the same Monte Carlo routine, but this time generating the random numbers according to the approximate distribution

$$\frac{1}{k(1 - \beta_e^2 \cos^2\Theta_\gamma)(1 - 2M_W^2/s - \beta_W \cos\Theta)}. \quad (4b)$$

The distribution (4b) develops singularities for low-energy photons, $k \rightarrow \omega$, for collinear photons, $|\cos\Theta_\gamma| \rightarrow 1$ and $\beta_e \rightarrow 1$ (i.e., $m_e^2 \ll s$), and finally, in the high-energy limit, where $M_W^2 \ll s$, also for a W^- boson collinear with a beam. The peaking structure (4a) and (4b) is approximately the same as that of the exact distributions.

As we shall discuss below, in the threshold region photonic corrections are large and dominated by the initial-state bremsstrahlung. Therefore it is important to take

into account the multiple-soft-photon emission and leading-logarithmic $O(\alpha^2)$ corrections on the initial-state side [18]. These QED corrections form a gauge-invariant subset, and the complete $O(\alpha^2)$ calculation of Berends *et al.* [19] is available for the s -channel-type diagrams. For the dominating t -channel diagram, such a calculation does not exist. We know that to one-loop order the virtual plus soft-photon corrections factorize in the usual way and for the hard part the Bonneau-Martin formula

$$\frac{d\sigma_{\text{Br}}}{dk} = \frac{2\alpha}{\pi} \left[\ln \frac{s}{m_e^2} - 1 \right] \frac{1+(1-k)^2}{k} \sigma_0(s(1-k))$$

applies. Similarly, the leading higher-order results obtained for the s -channel diagrams must apply for the t -channel contributions as well; otherwise, the gauge cancellation mechanism could not work any longer.

The initial-state photon emission changes the total cross section according to the convolution integral

$$\sigma_{\text{ini}}(s) = \int_0^{k_{\text{max}}} dk \rho_{\text{ini}}(k) \sigma_0(s(1-k)), \quad (5)$$

where $\rho_{\text{ini}}(k)$ is the photon radiation spectrum [18]. Here $k = E_\gamma/E_b$ is the photon energy in units of beam energy and $s' = s(1-k)$ is the effective s available for the W pair production after the photon has been emitted. $k_{\text{max}} = 1 - 4M_W^2/s$ is the maximum photon energy which in general will be given by an experimental cutoff.

The photon distribution function may be written in the form [19]

$$\rho_{\text{ini}}(k) = \beta k^{\beta-1} (1 + \delta_1^{v+s} + \delta_2^{v+s}) + \delta_1^h + \delta_2^h, \quad (6)$$

with $\beta = (2\alpha/\pi)(L-1)$, $L = \ln s/m_e^2$. The corrections are given by ($v+s$ = virtual + soft, h = hard)

$$\begin{aligned} \delta_1^{v+s} &= \frac{\alpha}{\pi} \left[\frac{3}{2}L + \frac{\pi^2}{3} - 2 \right], \\ \delta_2^{v+s} &= \left[\frac{\alpha}{\pi} \right]^2 \left[\left[\frac{9}{8} - \frac{\pi^2}{3} \right] L^2 + s_{21}L + s_{20} \right], \\ \delta_1^h &= \frac{\alpha}{\pi} (1-L)(2-k), \\ \delta_2^h &= \left[\frac{\alpha}{\pi} \right]^2 (h_{22}L^2 + h_{21}L + h_{20}), \end{aligned} \quad (7)$$

where

$$\begin{aligned} h_{22} &= -\frac{1+(1-k)^2}{k} \ln(1-k) \\ &\quad + (2-k) \left[\frac{1}{2} \ln(1-k) - 2 \ln k - \frac{3}{2} \right] - k \end{aligned}$$

and the other two-loop correction coefficients s_{2i} and h_{2i} are given in [19]. In the following we will take into account the leading-logarithmic $O(\alpha^2)$ terms only (i.e., set s_{21} , s_{20} , h_{21} , and h_{20} equal to zero).

Subdividing the $v+s$ part according to

$$\int_0^{k_{\text{max}}} dk \dots = \int_0^{k_0} dk \dots + \int_{k_0}^{k_{\text{max}}} dk \dots, \quad (8)$$

with $k_0 = \omega/E_b$, the first part corresponds to what is con-

ventionally called ‘‘exponentiation’’ [20] since

$$\int_0^{k_0} dk \beta k^{\beta-1} = k_0^\beta = e^{\beta \ln k_0}. \quad (9)$$

Up to first order in α , we obtain

$$k_0^\beta (1 + \delta_1^{v+s}) \sigma_0(s) \simeq (1 + \beta \ln k_0 + \delta_1^{v+s}) \sigma_0(s), \quad (10)$$

for the Born cross section corrected by the initial-state QED corrections. Subtracting this (unexponentiated) contribution from the full $O(\alpha)$ result and including (5) instead amounts to taking into account the additional higher-order corrections. It is clear that at higher energies, where the initial-state bremsstrahlung ceases to approximate well the full photonic corrections, our treatment of the leading $O(\alpha^2)$ terms is incomplete. However, the numerical results will show that (above the peak) the importance of the higher-order terms decreases as the energy increases. The approximation used here therefore should meet all requirements for comparison with future experiments.

III. RESULTS

The parameters used in our calculation are

$$M_Z = 91.176 \text{ GeV}, \quad M_W = 80.151 \text{ GeV}, \quad (11)$$

$$m_H = 100 \text{ GeV}, \quad m_t = 130 \text{ GeV}, \quad m_b = 4.5 \text{ GeV}.$$

For the light quarks, we use the effective masses

$$\begin{aligned} m_u &= 0.062 \text{ GeV}, \quad m_d = 0.083 \text{ GeV}, \\ m_c &= 1.5 \text{ GeV}, \quad m_s = 0.215 \text{ GeV}, \end{aligned} \quad (12)$$

and an effective QCD correction factor (see [21])

$$1 + 0.133/\pi. \quad (13)$$

This parametrization of the light-quark loops has been obtained by a fit (in the range $50 \text{ GeV} \leq \sqrt{s} \leq 200 \text{ GeV}$) of the hadronic contributions to the photon vacuum po-

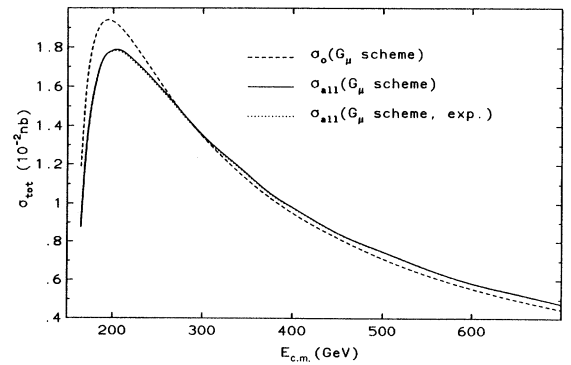


FIG. 2. Total cross section in lowest order (σ_0) and including radiative corrections (σ_{all}) in the G_μ scheme. The dotted line (exponentiated) represents the result obtained by adding multiple-soft-photon emission and leading-logarithmic $O(\alpha^2)$ corrections.

TABLE I. Numerical demonstration of the independence of the total cross section in the G_μ scheme on the soft-photon cutoff ($k_0 = \omega/E_b$); σ (10^{-2} nb). The results have been obtained with $M_Z = 91.176$ GeV and $M_W = 80.151$ GeV. The latter corresponds to $m_t = 130$ GeV and $m_H = 100$ GeV.

E (GeV)	k_0	σ_0	σ_{0+v+s}	σ_h	σ_{all}
170	10^{-2}	1.5521	0.9199	0.3293 ± 0.0002	1.2492
	10^{-3}		0.5179	0.7247 ± 0.0005	1.2426
	10^{-4}		0.1160	1.1259 ± 0.0008	1.2419
190	10^{-2}	1.9334	1.1179	0.6288 ± 0.0006	1.7466
	10^{-3}		0.6200	1.1251 ± 0.0011	1.7451
	10^{-4}		0.1220	1.6230 ± 0.0015	1.7450
200	10^{-2}	1.9318	1.1074	0.6805 ± 0.0008	1.7879
	10^{-3}		0.6108	1.1772 ± 0.0013	1.7881
	10^{-4}		0.1142	1.6736 ± 0.0017	1.7878
500	10^{-2}	0.7120	0.3888	0.3555 ± 0.0010	0.7443
	10^{-3}		0.2064	0.5367 ± 0.0013	0.7430
	10^{-4}		0.0239	0.7165 ± 0.0015	0.7404

larization, evaluated using the experimental e^+e^- annihilation data. This takes into account properly the leading light-quark contributions appearing in self-energy diagrams (running of α). For self-consistency, we use the same parametrization for the evaluation of the light-quark loops contributing to the ZWW and γWW form factors.

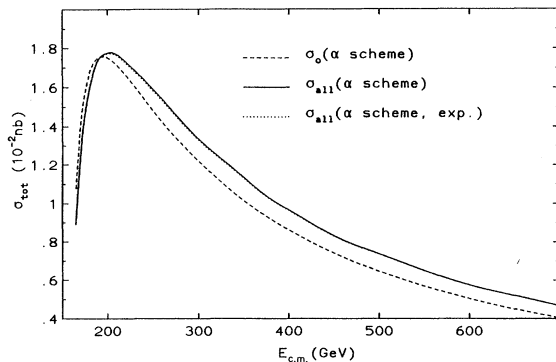
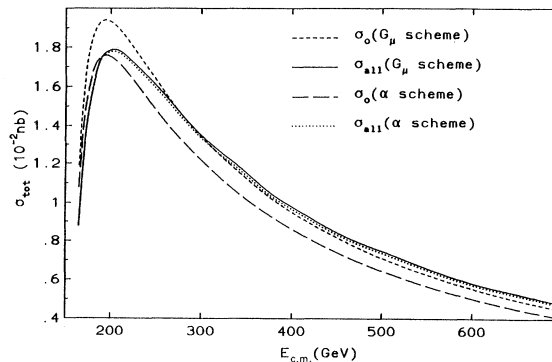
We have performed the calculation in the α and G_μ schemes. Apart from using different parametrizations, the renormalization in these two schemes differs also in the choice of the counterterms. As has been shown already in [8], the one-loop corrected results obtained in these two schemes differ only very little in spite of the fact that the Born cross sections differ considerably.

In Table I we show the independence of the total cross section on the soft-photon cutoff (for the G_μ scheme only). For $k_0 = \omega/E_b = 10^{-2}$, 10^{-3} , and 10^{-4} , Table I

shows the total cross section σ_{all} and its contributions σ_{0+v+s} and σ_h . In spite of the fact that the latter ones change by an order of magnitude, their sum σ_{all} changes by less than 0.5% with k_0 . The reason for the remaining discrepancy is threefold: first, the limited validity of the soft-photon approximation; second, the numerical stability of the MC integration decreases at higher energies; and third, the statistical error. For energies just above the threshold, photons carrying 0.01 of the beam energy cannot be considered as soft ones, and therefore the relative k_0 dependence gets bigger for lower energies. For higher energies the discrepancy increases because the integration range and peaking in the photon energy increases and in addition the peaking in the W production angle gets more pronounced. Concerning the statistical error, the errors shown in Table I are the ‘‘standard deviations’’ produced by the MC routine VEGAS [17]. These

TABLE II. Comparison of the results in the α and G_μ schemes. For each energy, the first line gives the $O(\alpha)$ result, and the second line includes the results from the exponentiation and $O(\alpha^2)$ leading logarithms. σ (10^{-2} nb), $k_0 = 10^{-4}$. The results have been obtained with $M_Z = 91.176$ GeV and $M_W = 80.151$ GeV. The latter corresponds to $m_t = 130$ GeV and $m_H = 100$ GeV.

E (GeV)	$\sigma_0(\alpha)$	$\sigma_{\text{all}}(\alpha)$	$\sigma_0(G_\mu)$	$\sigma_{\text{all}}(G_\mu)$
165	1.0793	0.8908 ± 0.0004	1.1904	0.8763 ± 0.0005
		0.9304		0.9199
170	1.4072	1.2535 ± 0.0007	1.5521	1.2419 ± 0.0008
		1.2790		1.2701
175	1.5803	1.4675 ± 0.0009	1.7430	1.4628 ± 0.0010
		1.4833		1.4802
180	1.6770	1.6031 ± 0.0011	1.8497	1.6030 ± 0.0012
		1.6121		1.6129
190	1.7529	1.7375 ± 0.0014	1.9334	1.7450 ± 0.0015
		1.7712		1.7457
200	1.7515	1.7748 ± 0.0015	1.9318	1.7878 ± 0.0017
		1.7712		1.7839
250	1.4836	1.5853 ± 0.0019	1.6364	1.6063 ± 0.0021
		1.5782		1.5985
300	1.2182	1.3333 ± 0.0018	1.3437	1.3530 ± 0.0021
		1.3278		1.3469
500	0.6455	0.7338 ± 0.0016	0.7120	0.7404 ± 0.0015
		0.7322		0.7386

FIG. 3. Same as Fig. 2 in the α scheme.FIG. 4. Comparison of the results in the α and G_μ schemes.

underestimate the real error considerably. The real relative error depends on the number N of calls to the integrand such as $1/\sqrt{N}$; i.e., with N of the order of 10^4 , as was used in our calculation, the error is expected to be of the order of 0.5–1.0%, which can also be seen by inspection of the examples given in Ref. [17].

Figures 2 and 3 represent our results in the G_μ and α schemes, respectively. By adding the hard bremsstrahlung, the trend of the correction differs from the one in Ref. [8] in so far as at higher energies (above the peak) the corrected total cross section is substantially larger than the Born cross section. This can be understood from Eq. (5). Since $\sigma_0(s)$ is decreasing and the observed cross section corresponds to the cross section at lower effective s , namely, $s' = s(1-k)$, we obtain a larger cross section due to hard-photon emission (a corresponding argument explains why the cross section gets decreased below the peak). In addition, with growing energy the phase space for hard photons grows, which also increases the cross section. In Figs. 2 and 3 we also show the change of the results due to the inclusion of the higher-order effects (exponentiation), obtained by replacing the $O(\alpha)$ QED-corrected cross section (10) by the convolution integral (5). Above 180 GeV the difference turns out to be below 0.5% and changes sign at above 191 GeV. Approaching the threshold from above, these effects

grow to 17% at 160.5 GeV, 32% at 160.32 GeV, and 68% at 0.1 MeV above threshold (160.302 GeV). Table II gives numerical values for the cross section in the two schemes, including corrections due to exponentiation, and Fig. 4 finally shows the comparison of the α and G_μ schemes, which demonstrates the excellent agreement of the results in the two schemes. All calculations have finally been performed with $k_0 = 10^{-4}$.

We have checked that the soft-photon approximation used in Ref. [8], for example, for $k_0 = 0.1$ overestimates the correction by 1% at 200 GeV and by 0.4% at 500 GeV. To the accuracy we are aiming at, this commonly used approximation is valid only if k_0 does not exceed 0.01.

It is also interesting to note that the difference between the complete hard bremsstrahlung and the initial-state hard bremsstrahlung increases from small values (-0.3% at 165 GeV) in the threshold region to -2.1% at 200 GeV and -11.2% at 500 GeV. Thus taking into account the initial-state bremsstrahlung only is not a sufficiently good approximation even at LEP 200 energies.

In Figs. 5 and 6 we also present results for various cuts in the photon phase space. Such cuts will be relevant for more realistic experimental setups. Figure 5 shows re-

TABLE III. Comparison of σ_{all} in the G_μ scheme with the results of Ref. [11]. The parameters are the same as in Ref. [11]; the units are the same as in Tables I and II. $M_Z = 91.17$ GeV and $M_W = 80.287$ GeV, the latter corresponding to $m_t = 150$ GeV and $m_H = 100$ GeV.

E (GeV)	$\sigma_0(G_\mu)$	$\sigma_{\text{all}}(\alpha)$	$\sigma_{\text{all}}(G_\mu)$ (Ref. [11])	σ^I	σ^{II}	$\sigma_{\text{all}}(G_\mu)$ (present work)
165	1.1649	0.8656	0.8455	0.8438	0.8462	0.8506
170	1.5421	1.2425	1.2221	1.2227	1.2250	1.2307
175	1.7399	1.4641	1.4449	1.4476	1.4495	1.4558
180	1.8504	1.6044	1.5899	1.5913	1.5929	1.5995
190	1.9381	1.7444	1.7369	1.7366	1.7378	1.7445
200	1.9382	1.7843	1.7820	1.7803	1.7810	1.7875
250	1.6438	1.5974	1.6033	1.6018	1.6016	1.6067
300	1.3502	1.3452	1.3526	1.3519	1.3514	1.3556
500	0.7158	0.7419	0.7398	0.7482	0.7476	0.7497

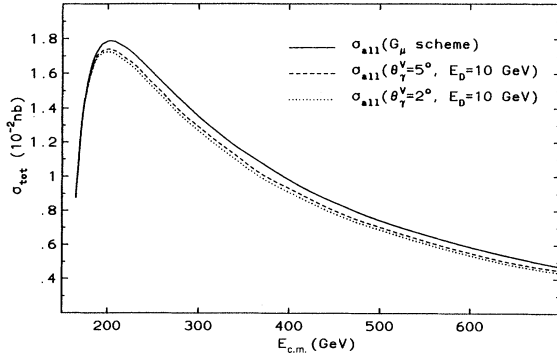


FIG. 5. Total cross section with cut (E_D) in the photon energy (G_μ scheme).

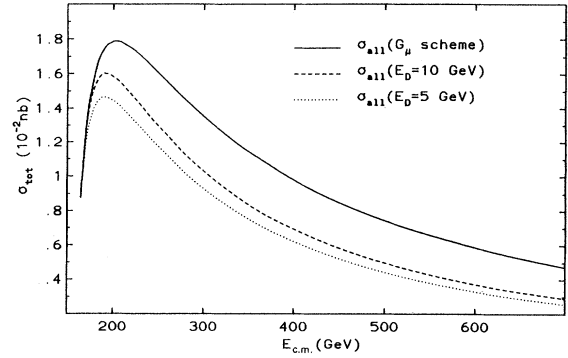


FIG. 6. Same as Fig. 5 with an angular cut (Θ_γ^V) for $E_D=10$ GeV.

sults for cuts in the photon energy $|\mathbf{k}| \leq E_D$, $E_D=5$ and 10 GeV, respectively, compared with σ_{all} without any cut. Indeed, cuts of this magnitude have a very stringent effect by reducing the cross sections considerably. The effects are not so severe for angular cuts of $\Theta_\gamma^V=5^\circ$ and 2° as indicated in Fig. 6.

Finally, in Table III we compare the results of Beenakker, Kołodziej, and Sack [11] with the ones we obtain for the same set input parameters. In Ref. [11] the calculation was done in the α scheme together with a resummation of the fermionic contribution to the W wave-function renormalization which is the dominating correction [12]. For the parameter values used here, $\Delta w_f = -0.0473$. If we use the same resummation, we obtain the result

$$\sigma^I = [\sigma(\alpha) + 2\Delta w_f \sigma_0(\alpha)] \left[\frac{1}{1 + \Delta w_f} \right]^2.$$

These results agree well. Up to nonleading $O(\alpha^2)$ terms, σ^I is equivalent to

$$\sigma^{II} = [\sigma(\alpha) - 2\Delta r \sigma_0(\alpha)] \left[\frac{1}{1 - \Delta r} \right]^2,$$

where $\Delta r = 0.0395$, which relates the α to the G_μ scheme. The two summation procedures yield results which differ by $(\sigma^I - \sigma^{II})/\sigma_0(\alpha) = -0.0028$ at $E = 165$ GeV, increasing monotonically to 0.0007 at $E = 500$ GeV. In our calculation we use G_μ not only in calculating the Born cross section, but also in calculating the non-QED correction. This yields a slightly smaller correction $[\sigma^{II} - \sigma(G_\mu)]/\sigma_0(G_\mu) = -0.0053$ at $E = 165$ GeV, increasing monotonically to -0.0028 at $E = 500$ GeV. The differences arise from a different treatment of the higher-order effects and thus are a measure for the miss-

ing higher-order contributions (scheme dependence). While below 500 GeV the discrepancy between σ^I and Ref. [11] is at most 0.2%, there is a 1% discrepancy at 500 GeV, which probably cannot be explained as a statistical fluctuation.

In this paper we have treated the W 's as stable on-shell particles. This approximation is insufficient for a careful investigation of the threshold region (W mass measurement). Since the W particles are very short lived, the process actually observed is $e^+e^- \rightarrow 4f$ (four fermions). Although the corresponding cross section is dominated by $e^+e^- \rightarrow W^+W^- \rightarrow 4f$ where both W 's are at resonance, there is an observable deviation also above the $2M_W$ threshold (see, e.g., Ref. [22]). Recently, in Ref. [23], the hard bremsstrahlung for $e^+e^- \rightarrow 4f$ was calculated. The cross section in the LEP 200 energy range is increased by about 5% above the on-shell W threshold ($2M_W$). Experimental cuts which require both W 's to be close to "on shell" may reduce the cross section by essentially the same amount. The precise reduction factor, of course, can only be calculated by a study of such cuts using a full $e^+e^- \rightarrow 4f, 4f\gamma$ MC event generator. Furthermore, there are indications [24] that background processes such as $e^+e^- \rightarrow W^+e^-\nu_e$ (where the $e^-\nu_e$ pair is not a decayed W^-) may not be completely ignored in a precise calculation of the threshold behavior.

ACKNOWLEDGMENTS

We are very much indebted to G. van Oldenborgh for providing us with the FORTRAN routines for the numerical calculation of the scalar one-loop integrals. We also thank A. Aeppli for the routines which calculate the tensor integrals in terms of the scalar one-loop integrals. K.K. was supported in part by the Alexander von Humboldt Foundation.

[1] O. P. Sushkov, V. V. Flambaum, and I. B. Khriplovick, *Yad. Fiz.* **20**, 1016 (1975) [*Sov. J. Nucl. Phys.* **20**, 537 (1975)]; W. Alles, Ch. Boyer, and A. J. Buras, *Nucl. Phys.* **B119**, 125 (1977); J. K. F. Gaemers and G. J. Gounaris, *Z. Phys. C* **1**, 259 (1979); K. Hagiwara, R. D. Peccei, D. Zepfenfeld, and K. Hikasa, *Nucl. Phys.* **B282**, 253 (1987).

[2] J. Carter, in *Proceedings of the Joint International Lepton-Photon Symposium and Europhysics Conference on High Energy Physics*, Geneva, Switzerland, 1991, edited by S. Hegarty, K. Potter, and E. Quercigh (World Scientific, Singapore, 1992).

[3] G. Burgers and F. Jegerlehner, in *Z Physics at LEP 1*,

- Proceedings of the Workshop, Geneva, Switzerland, 1989, edited by G. Altarelli *et al.* (CERN Report No. 89-08, Geneva, 1989); Z. Hioki, *Z. Phys. C* **49**, 287 (1991).
- [4] H. Plathow-Besch, in *Proceedings of the Joint International Lepton-Photon Symposium and Europhysics Conference on High Energy Physics* [2].
- [5] M. Lemoine and M. Veltman, *Nucl. Phys.* **B164**, 445 (1980).
- [6] R. Philippe, *Phys. Rev. D* **26**, 1588 (1982).
- [7] M. Böhm, A. Denner, T. Sack, W. Beenakker, F. Berends, and H. Kuijf, *Nucl. Phys.* **B304**, 463 (1988).
- [8] J. Fleischer, F. Jegerlehner, and M. Zraček, *Z. Phys. C* **42**, 409 (1989).
- [9] F. M. Renard, *Z. Phys. C* **2**, 17 (1979).
- [10] K. Kołodziej and M. Zraček, *Phys. Rev. D* **43**, 3619 (1991).
- [11] W. Beenakker, K. Kołodziej, and T. Sack, *Phys. Lett. B* **258**, 469 (1991). Previously, in Ref. [13] the hard bremsstrahlung part was calculated and combined with the virtual and soft-photon results of Ref. [8] using tables presented in Ref. [14]. Here the aim is to present a complete calculation as in Ref. [11].
- [12] T. Sack (private communication).
- [13] H. Tanaka, T. Kaneko, and Y. Shimizu, *Comput. Phys. Commun.* **64**, 149 (1991).
- [14] F. Jegerlehner, in *Radiative Corrections for e^+e^- Colliders*, edited by J. H. Kühn (Springer, Berlin, 1989).
- [15] F. A. Berends and W. T. Giele, *Nucl. Phys.* **B306**, 759 (1988); **B313**, 595 (1989); F. A. Berends, W. T. Giele, and H. Kuijf, *Phys. Lett. B* **232**, 266 (1989); *Nucl. Phys.* **B321**, 39 (1989); **B333**, 120 (1990).
- [16] F. Jegerlehner, in *Radiative Corrections, Results and Perspectives*, edited by N. Dombey and F. Boudjema (Plenum, New York, 1990).
- [17] G. P. Lepage, *J. Comput. Phys.* **27**, 192 (1978); Cornell University Report No. CLNS-80/447, 1980 (unpublished).
- [18] G. Bonneau and F. Martin, *Nucl. Phys.* **B27**, 381 (1971); M. Greco, G. Pancheri, and Y. Srivastava, *ibid.* **B171**, 118 (1980); **B197**, 543(E) (1982); F. A. Berends, R. Kleiss, and S. Jadach, *ibid.* **B202**, 63 (1982); M. Böhm and W. Hollik, *ibid.* **B204**, 45 (1982).
- [19] F. A. Berends, G. Burgers, and W. L. van Neerven, *Phys. Lett. B* **177**, 191 (1986); *Nucl. Phys.* **B297**, 429 (1988); **B304**, 921(E) (1988); F. A. Berends, in *Radiative Corrections for e^+e^- Colliders* [14]; F. A. Berends *et al.*, in *Z Physics at LEP 1*, [3].
- [20] D. R. Yennie, S. C. Frautschi, and H. Suura, *Ann. Phys. (N.Y.)* **13**, 379 (1961); D. R. Yennie, *Phys. Rev. Lett.* **34**, 239 (1975); J. D. Jackson and D. L. Scharre, *Nucl. Instrum. Methods* **128**, 13 (1975); M. Greco, G. Pancheri, and Y. Srivastava, *Nucl. Phys.* **B101**, 234 (1975); S. Jadach and B. F. L. Ward, *Phys. Rev. D* **38**, 2897 (1988); **42**, 1404 (1990).
- [21] F. Jegerlehner, in *Testing the Standard Model*, edited by M. Cvetič and P. Langacker (World Scientific, Singapore, 1991), p. 569.
- [22] J. F. Gunion and Z. Kunszt, *Phys. Rev. D* **33**, 665 (1986).
- [23] A. Aeppli and D. Wyler, *Phys. Lett. B* **262**, 125 (1991).
- [24] J. C. Romão and P. Nogueira, *Z. Phys. C* **42**, 263 (1989).